DOI:10.1093/jnci/dju113
First published online June 6, 2014

ARTICLE

Effects of a Novel Long Noncoding RNA, lncUSMycN, on N-Myc Expression and Neuroblastoma Progression

Pei Y. Liu, Daniela Erriquez, Glenn M. Marshall, Andrew E. Tee, Patsie Polly, Mathew Wong, Bing Liu, Jessica L. Bell, Xu D. Zhang, Giorgio Milazzo, Belamy B. Cheung, Archa Fox, Alexander Swarbrick, Stefan Hüttelmaier, Maria Kavallaris, Giovanni Perini, John S. Mattick, Marcel E. Dinger, Tao Liu

Manuscript received December 16, 2013; revised March 14, 2014; accepted March 27, 2014.

Correspondence to: Tao Liu, BMed, PhD, Children's Cancer Institute Australia for Medical Research, Lowy Cancer Research Centre, University of New South Wales, PO Box 81, Randwick, NSW 2031, Australia (e-mail: tliu@ccia.unsw.edu.au).

Background Patients with neuroblastoma due to the amplification of a 130-kb genomic DNA region containing the *MYCN* oncogene have poor prognoses.

Methods Bioinformatics data were used to discover a novel long noncoding RNA, lncUSMycN, at the 130-kb amplicon. RNA-protein pull-down assays were used to identify proteins bound to lncUSMycN RNA. Kaplan–Meier survival analysis, multivariable Cox regression, and two-sided log-rank test were used to examine the prognostic value of lncUSMycN and NonO expression in three cohorts of neuroblastoma patients (n = 47, 88, and 476, respectively). Neuroblastoma-bearing mice were treated with antisense oligonucleotides targeting lncUSMycN (n = 12) or mismatch sequence (n = 13), and results were analyzed by multiple comparison two-way analysis of variance. All statistical tests were two-sided.

Results Bioinformatics data predicted lncUSMycN gene and RNA, and reverse-transcription polymerase chain reaction confirmed its three exons and two introns. The *lncUSMycN* gene was coamplified with *MYCN* in 88 of 341 human neuroblastoma tissues. lncUSMycN RNA bound to the RNA-binding protein NonO, leading to N-Myc RNA upregulation and neuroblastoma cell proliferation. High levels of lncUSMycN and NonO expression in human neuroblastoma tissues independently predicted poor patient prognoses (lncUSMycN: hazard ratio [HR] = 1.87, 95% confidence interval [CI] = 1.06 to 3.28, $P = .03$; NonO: HR = 2.48, 95% CI = 1.34 to 4.57, $P = .004$). Treatment with antisense oligonucleotides targeting lncUSMycN in neuroblastoma-bearing mice statistically significantly hindered tumor progression ($P < .001$).

Conclusions Our data demonstrate the important roles of lncUSMycN and NonO in regulating N-Myc expression and neuroblastoma oncogenesis and provide the first evidence that amplification of long noncoding RNA genes can contribute to tumorigenesis.

JNCI J Natl Cancer Inst (2014) 106(7): dju113 doi:10.1093/jnci/dju113

Cancer is the most common cause of death from disease in children, and neuroblastoma is the most common solid tumor in early childhood. Amplification of a 130-kb core genomic DNA region containing the *MYCN* oncogene is a clonal feature in 25% to 30% of human neuroblastoma tissues (1). Myc oncoproteins, including N-Myc and c-Myc, induce cell proliferation, malignant transformation, and tumor progression (2–4).

At least 90% of the human genome is transcribed to generate an extraordinary range of non-protein-coding (noncoding) RNAs, including long noncoding RNAs (lncRNAs) (5–7). Although more than 10 000 human lncRNAs have been predicted by bioinformatics analyses or identified by cDNA/RNA sequencing analyses, less than 1% have been experimentally characterized (7–9). Recent studies have demonstrated that the expression of lncRNAs is regulated by key transcription factors (7,10) and by biological processes such as cell differentiation (11) and that lncRNAs play key roles in cancer cell proliferation, survival, invasion, and metastasis by regulating gene expression (10,12–17).

Although the *MYCN* oncogene has been extensively studied in the last three decades, it is unknown whether other genomic elements within the 130-kb amplicon containing *MYCN* play a role in neuroblastoma tumorigenesis. Here we identified a novel lncRNA upstream of *MYCN*, lncUSMycN, transcribed from the 130-kb amplicon, and found that lncUSMycN upregulated N-Myc mRNA expression by binding to NonO protein.

Methods

Experimental Therapy

Animal experiments were approved by the Animal Care and Ethics Committee of the University of New South Wales, Australia, and the animals' care was in accord with institutional guidelines. Female

Balb/c mice aged 5 to 6 weeks were injected subcutaneously with 10^7 Kelly human neuroblastoma cells into the flanks. When tumors reached 0.05 g, the mice were injected intraperitoneally with locked nucleic acid (LNA)–antisense oligonucleotide (LNA-ASO) targeting lncUSMycN (lncUSMycN LNA-ASO) or control LNA-ASO at 50 mg/kg every second day for 2 weeks. Tumor mass was measured and calculated. The mice were killed at the end of the 14-day therapy, and tumor tissues were collected, weighed, formalin fixed, and paraffin embedded for immunohistochemistry analysis.

Patient Tumor Sample Analysis

Forty-seven primary neuroblastoma cDNA samples synthesized from tumors from untreated patients were obtained from Children's Cancer Institute Australia and had been studied previously (Supplementary Table 1, available online) (18). The study was approved by Sydney Children's Hospitals Network Human Research Ethics Committee, and written informed consent was waived because samples were collected before 2003. The International Neuroblastoma Staging System (22) was used to classify disease stage. Sex and racial/ethnic groups were not analyzed because they were not prognostic factors for neuroblastoma (22).

lncUSMycN, NonO, and N-Myc expression in neuroblastoma tissues were also analyzed in 88 (Versteeg dataset) and 476 (Kocak dataset) human neuroblastoma samples in the publically available gene expression databases (http://r2.amc.nl, last accessed August 26, 2013). Clinical information for the 88 patients in the Versteeg dataset was directly downloaded from http://r2.amc.nl, last accessed August 26, 2013, and clinical information for the 476 patients in the Kocak dataset was obtained from the authors' previous publications (19,20).

Statistical Procedures

Experiments were repeated at least three times. All data for statistical analysis were calculated as mean ± standard deviation (SD). Differences were analyzed for statistical significance using two-sided unpaired *t* test for two groups or multiple comparison one-way or two-way analysis of variance (ANOVA) for more than two groups.

Correlation between N-Myc expression and lncUSMycN or NonO expression in human neuroblastoma tissues was examined with Pearson's correlation. For patient prognosis studies, overall survival was defined as the time from diagnosis until death or until last contact if the patient did not die. The patient cohort was dichotomized into two groups (low vs high lncUSMycN or NonO expression) on the basis of the median or high decile value of lncUSMycN or NonO in the cohort. Survival analyses were performed according to the method of Kaplan and Meier, and comparisons of survival curves were made using two-sided log-rank tests (21). Multivariable Cox regression analyses were performed to determine whether lncUSMycN and NonO expression in human neuroblastoma tissues predicted patient prognosis independent of patient age, disease stage (22), and *MYCN* gene amplification status. Probabilities of survival and hazard ratios (HRs) were provided with 95% confidence intervals (CIs). Proportionality was confirmed by visual inspection of the plots of log(2log(S(time))) vs log(time), which were observed to remain parallel.

A probability value of .05 or less was considered statistically significant. All statistical tests were two-sided.

Additional methods are provided as Supplementary Methods (available online).

Results

Identification of Full-Length lncUSMycN RNA

By extracting bioinformatics data generated by the HAVANA team at the Sanger Institute, we found a novel lncRNA upstream of *MYCN*, which we named lncUSMycN, within the 130-kb amplicon containing the *MYCN* oncogene (Figure 1A; Supplementary Figure 1A, available online). To identify the full-length lncUSMycN RNA, we first performed reverse-transcription polymerase chain reaction (RT-PCR) with primers targeting the beginning of exon 1 and the end of exon 3. Sequencing analysis revealed that the PCR product matched the 3 exons of lncUSMycN without incorporation of the two introns (Figure 1B; Supplementary Figure 1A, available online). We then performed rapid amplification of cDNA ends (RACE) PCR to amplify the 5' and 3' ends of lncUSMycN. Sequencing of the RACE PCR products revealed an extra 140-bp sequence upstream of the first exon (Supplementary Figure 1B, available online).

To confirm that *lncUSMycN* does not encode a protein, we cloned the full-length lncUSMycN into pcDNA3.1+ construct and performed in vitro translation assays. The assays showed that lncUSMycN did not have protein-coding potential, whereas positive control tissue transglutaminase and T7 expression constructs gave rise to proteins (Figure 1C).

We next used the publically available single nucleotide polymorphism array data from human neuroblastoma tissues, which were originally generated by the Therapeutically Applicable Research to Generate Effective Treatments initiative (https://target-data.nci.nih.gov/, last accessed June 12, 2013). Gene copy number analysis revealed that *MYCN* amplification was observed in 89 of 341 (26.1%) samples for data which passed quality control, whereas *lncUSMycN* was amplified in 88 of the 341 (25.8%) samples (Supplementary Tables 2 and 3, available online). Importantly, although all the *lncUSMycN* gene-amplified neuroblastoma tissues displayed *MYCN* gene amplification, only one of the 89 *MYCN*-amplified tumor tissues did not show concomitant *lncUSMycN* amplification.

We next examined *lncUSMycN* expression in human neuroblastoma cell lines and tumor tissues. RT-PCR analyses showed that lncUSMycN RNA was expressed in the *MYCN*-amplified IMR32, BE2C, SK-N-DZ, CHP134, and Kelly neuroblastoma cells but was undetectable in *MYCN* nonamplified SK-N-FI, SK-N-AS, NB69, SY5Y, and SHEP, as well as *MYCN*-amplified LAN-1 neuroblastoma cells (Figure 1D, available online). Furthermore, RT-PCR analysis of 47 human neuroblastoma tissues (Supplementary Table 1, available online) showed that lncUSMycN RNA was detectable in nine of 10 *MYCN*-amplified, but only four of 37 *MYCN* nonamplified, human neuroblastoma tissues (Figure 1E). Taken together, the data confirm that the *lncUSMycN* gene is frequently coamplified with *MYCN* and that lncUSMycN RNA is overexpressed in *MYCN* oncogene-amplified human neuroblastoma cell lines and tumor tissues.

Effect of lncUSMycN on N-Myc Expression

lncRNAs are well-known to regulate the expression of neighboring protein-coding genes (11,14,29). We therefore examined whether lncUSMycN regulated N-Myc expression. As shown in Figure 2, transfection with lncUSMycN siRNA-1 or lncUSMycN siRNA-2 knocked down lncUSMycN expression (Figure 2A), reduced

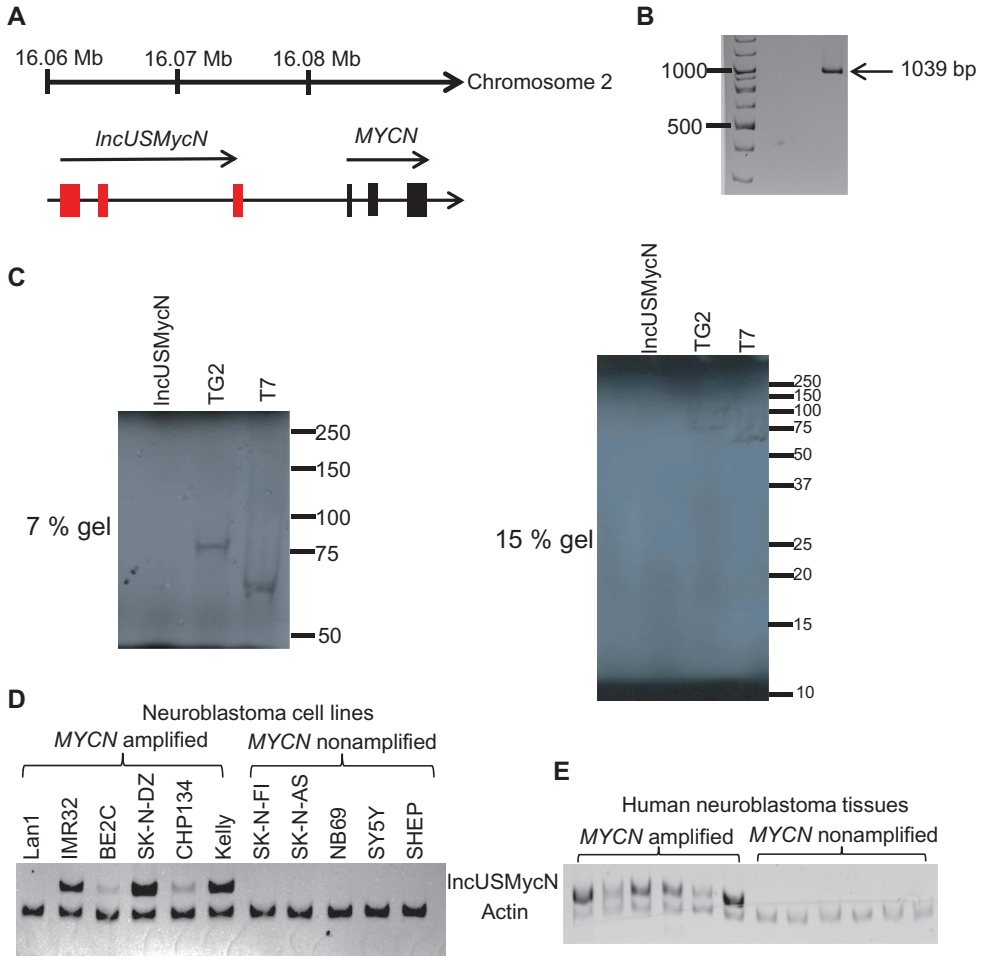

Figure 1. Identification of full-length lncUSMycN RNA. **A**) Schematic representation of the *lncUSMycN* gene and the *MYCN* gene at the forward strand of chromosome 2, as predicted by the HAVANA team. **B**) RNA was extracted from SK-N-DZ neuroblastoma cells and subjected to reverse-transcription polymerase chain reaction (RT-PCR) studies with primers targeting the beginning of exon 1 and the end of exon 3 of lncUSMycN predicted by the HAVANA team. The RT-PCR products were separated by agarose gel electrophoresis. **C**) In vitro translation assays were performed by mixing rabbit reticulocyte lysate, reaction buffer, T7 RNA polymerase, amino acid mixture minus Methionine, EasyTag L-[35S]-methionine, and pcDNA3.1+ construct expressing lncUSMycN, the positive control tissue transglutaminase (TG2) or T7. Translation products were separated using 7% and 15% sodium dodecyl sulfate polyacrylamide gel electrophoresis (SDS-PAGE) gels, and detected by autoradiography. **D**) RT-PCR studies were performed in six *MYCN*-amplified and five *MYCN*-nonamplified human neuroblastoma cell lines with primers targeting lncUSMycN or the housekeeping gene actin. **E**) RT-PCR studies were performed in 47 human neuroblastoma cDNA samples with primers targeting lncUSMycN or the housekeeping gene actin. A representative gel is shown.

N-Myc protein expression, and reduced N-Myc mRNA expression in BE2C cells (mean fold of control siRNA ± SD: N-Myc siRNA-1, 0.67 ± 0.11; N-Myc siRNA-2, 0.60 ± 0.04; $P < .01$, one-way ANOVA) and Kelly cells (mean fold of control siRNA ± SD: N-Myc siRNA-1, 0.66 ± 0.07; N-Myc siRNA-2, 0.53 ± 0.04; $P < .01$, one-way ANOVA) (Figure 2B). Consistently, ectopic expression of lncUSMycN upregulated exogenous N-Myc mRNA (mean fold of control ± SD: empty vector plus N-Myc construct, 93 349 ± 13 028; lncUSMycN construct plus N-Myc construct, 145 233 ± 12 335; $P < .01$, two-sided *t* test) and protein in *MYCN* nonamplified SK-N-AS cells (Figure 2C).

To understand whether lncUSMycN upregulated N-Myc expression through activation of *MYCN* gene transcription, we performed chromatin immunoprecipitation assays with a control antibody or an antibody against trimethylated histone H3 lysine 4 (H3K4me3 Ab), a marker for active gene transcription. As shown in Figure 2, D and E, the chromatin immunoprecipitation assays demonstrated that knocking down lncUSMycN expression with siRNAs did not reduce the presence of H3K4me3 at the *MYCN* gene promoter. Moreover, luciferase assays showed that lncUSMycN did not modulate *MYCN* promoter activity (Supplementary Figure 2, available online). Taken together, the data indicate that lncUSMycN upregulates N-Myc expression through a post-transcriptional mechanism.

lncUSMycN in Neuroblastoma Cell Proliferation and as a Prognostic Marker

We next investigated whether lncUSMycN was differentially expressed at different phases of the cell cycle and regulated cell proliferation. BE2C neuroblastoma cells were synchronized at G_0, G_1, G_1/S, S, G_2/M, or mitosis phase as we described previously (30). As shown in Figure 3A, lncUSMycN RNA was expressed at the lowest in cells at G0 phase and the highest in cells at G1/S and S phases. Alamar blue assays showed that lncUSMycN siRNAs reduced the numbers of viable Kelly

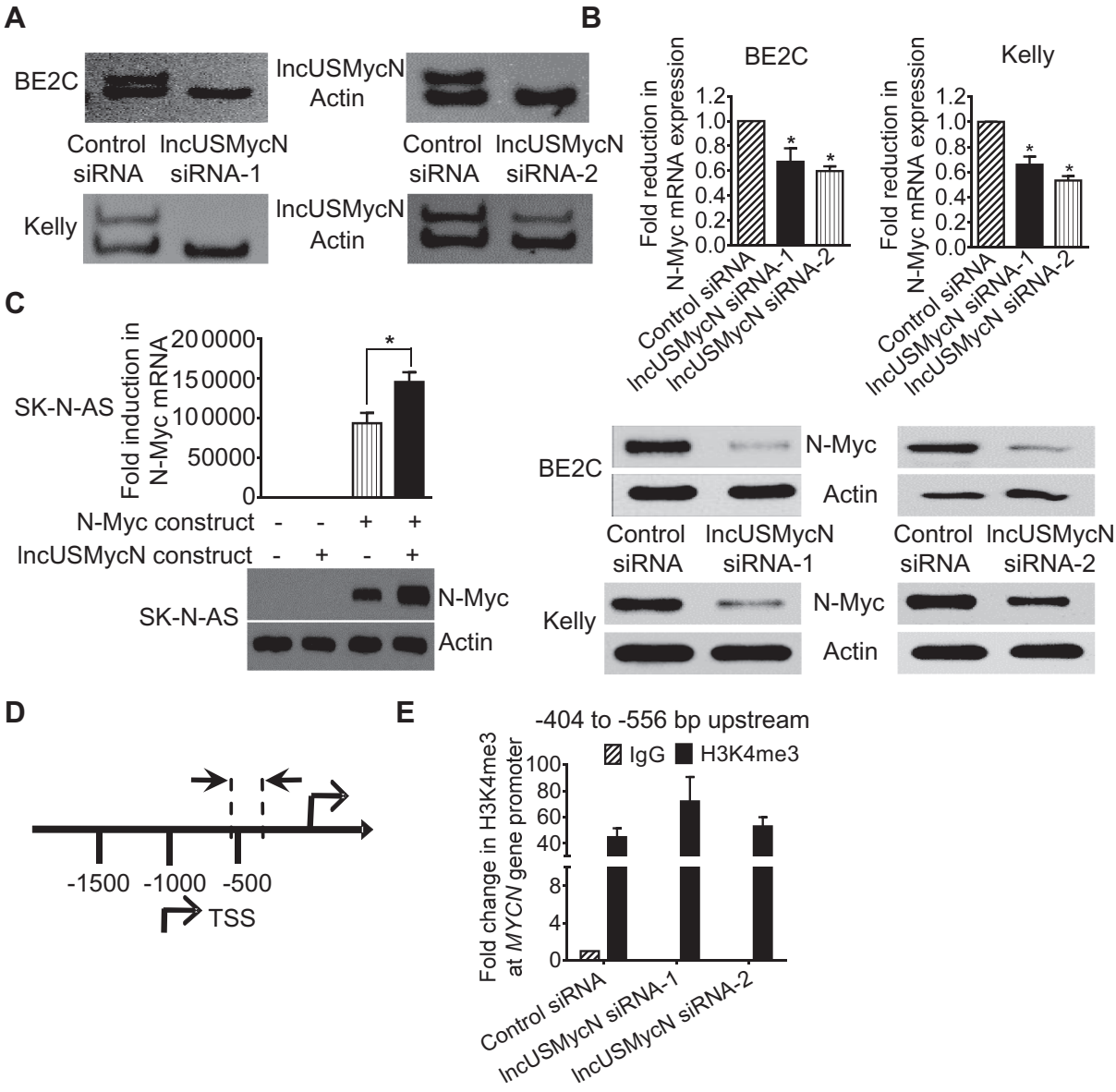

Figure 2. Effect of lncUSMycN on N-Myc expression. **A** and **B**) Kelly and BE2C cells were transfected with control siRNA, lncUSMycN siRNA-1, or lncUSMycN siRNA-2 for 48 hours, followed by reverse-transcription polymerase chain reaction (RT-PCR) analysis of lncUSMycN expression (**A**) as well as RT-PCR and immunoblot analysis of N-Myc expression (**B**). One-way analysis of variance was used to determine statistical significance. **C**) SK-N-AS cells were cotransfected with an empty vector, an lncUSMycN expression construct, and/or an N-Myc expression construct for 48 hours, followed by RT-PCR and immunoblot analysis of N-Myc expression. Two-sided *t* test was used to determine statistical significance. **D**) Schematic representation of the *MYCN* gene promoter. TSS represented transcription start site. **E**) Chromatin immunoprecipitation assays were performed with a control antibody or an anti-trimethyl-H3K4 (H3K4me3) antibody and real-time PCR with primers targeting proximal *MYCN* promoter region (–404 to –556 bp upstream of the *MYCN* gene transcription start site) in Kelly cells after transfection with control siRNA, lncUSMycN siRNA-1, or lncUSMycN siRNA-2. Fold change in the presence of H3K4me3 at the *MYCN* gene promoter region was obtained after dividing fold enrichment of H3K4me3 at the *MYCN* gene promoter region by fold enrichment of H3K4me3 at the control gene promoter region. Fold enrichment by the control antibody was artificially set as 1.0. Error bars represent standard deviation. **P* < .01.

and BE2C cells (Figure 3B) but did not reduce the numbers of viable SK-N-AS cells (Figure 3C), which did not express N-Myc and lncUSMycN. Additionally, flow cytometry analysis of the cell cycle showed that knocking down lncUSMycN expression with siRNAs had minimal effect in increasing the percentage of cells at G0 phase (Supplementary Figure 3, available online). Taken together, the data suggest that lncUSMycN induces neuroblastoma cell proliferation.

We showed in Figure 1 that lncUSMycN expression in a cohort of 47 human neuroblastoma tissues associated with N-Myc expression. Kaplan–Meier analysis showed that patients with neuroblastoma tissues exhibiting high levels of lncUSMycN expression had poor survival rates (HR = 4.29; 95% CI = 1.46 to 24.79; *P* = .01) (Figure 3D). Additionally, analyses of the publically available (http://r2.amc.nl, last accessed August 26, 2013) Versteeg and Kocak (19,20) microarray gene expression datasets revealed that lncUSMycN expression in tumor tissues positively correlated with N-Myc expression in cohorts of 88 and 476 neuroblastoma patients, respectively (Versteeg dataset: *R* = 0.227,

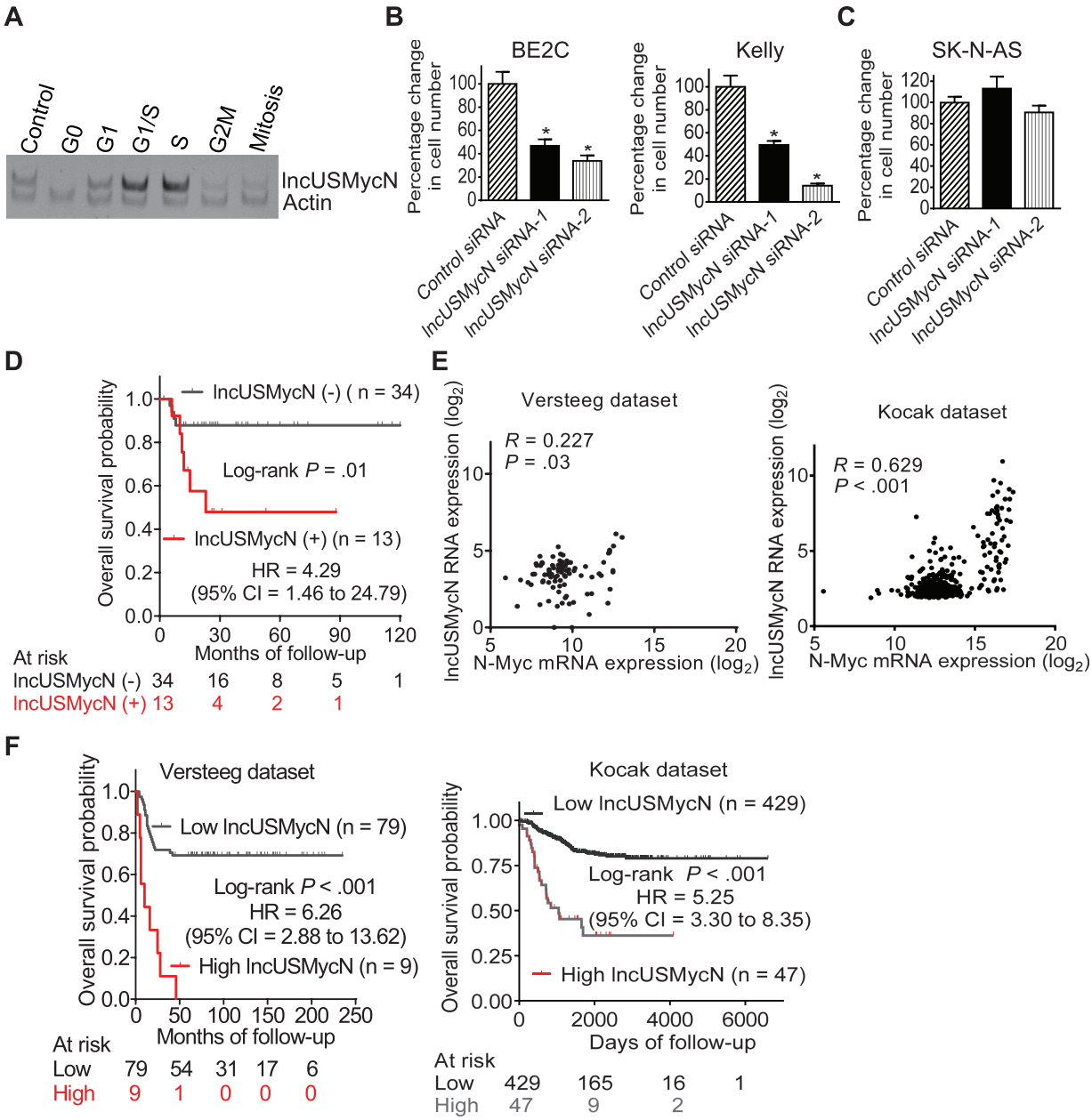

Figure 3. lncUSMycN in neuroblastoma cell proliferation and as a prognostic marker. **A**) BE2C neuroblastoma cells were synchronized at G0 phase by serum starvation, G1 phase by 3 hours in complete culture medium after serum starvation, the G1/S boundary by treatment with aphidicolin for 16 hours, S phase by 3 hours after aphidicolin release, the G2/M boundary by treatment with nocodazole for 16 hours, mitosis phase by 1 hour after nocodazole release. The expression of lncUSMycN at different phases of the cell cycle was analysed by reverse-transcription polymerase chain reaction (RT-PCR). **B** and **C**) Kelly, BE2C (**B**) and SK-N-AS (**C**) cells were transfected with control siRNA, lncUSMycN siRNA-1, or lncUSMycN siRNA-2 for 96 hours. Relative cell numbers were examined by Alamar blue assays and expressed as percentage changes in cell numbers. One-way analysis of variance was used to determine statistical significance. **D**) RT-PCR studies were performed in 47 human neuroblastoma cDNA samples with primers targeting lncUSMycN. Kaplan–Meier curves showed the probability of overall survival according to the level of lncUSMycN expression in the 47 neuroblastoma patients. *P* value was obtained from two-sided log-rank test. **E**) Two-sided Pearson's correlation was used to analyze correlation between lncUSMycN expression and N-Myc expression in tumor tissues from 88 and 476 neuroblastoma patients in the publically available microarray gene expression Versteeg dataset and Kocak dataset, respectively, which were downloaded from R2 microarray analysis and visualization platform (http://r2.amc.nl, last accessed August 26, 2013). **F**) Kaplan–Meier curves showed the probability of overall survival of patients according to the level of lncUSMycN expression in the 88 and 476 neuroblastoma patients in the Versteeg and Kocak datasets, respectively. CI = confidence interval; HR = hazard ratio. *P* value was obtained from two-sided log-rank test. Error bars represent standard deviation. **P* < .001.

95% CI = 0.018 to 0.417, $P = .03$; Kocak dataset: $R = 0.629$, 95% CI = 0.571 to 0.680, $P < .001$) (Figure 3E). Using the upper decile of lncUSMycN expression as the cutoff point, Kaplan–Meier analysis showed that high levels of lncUSMycN RNA expression in human neuroblastoma tissues positively associated with poor patient prognoses (Versteeg dataset: HR = 6.26, 95% CI = 2.88 to 13.62, $P < .001$; Kocak dataset, HR = 5.25, 95% CI = 3.30 to 8.35, $P < .001$) (Figure 3F).

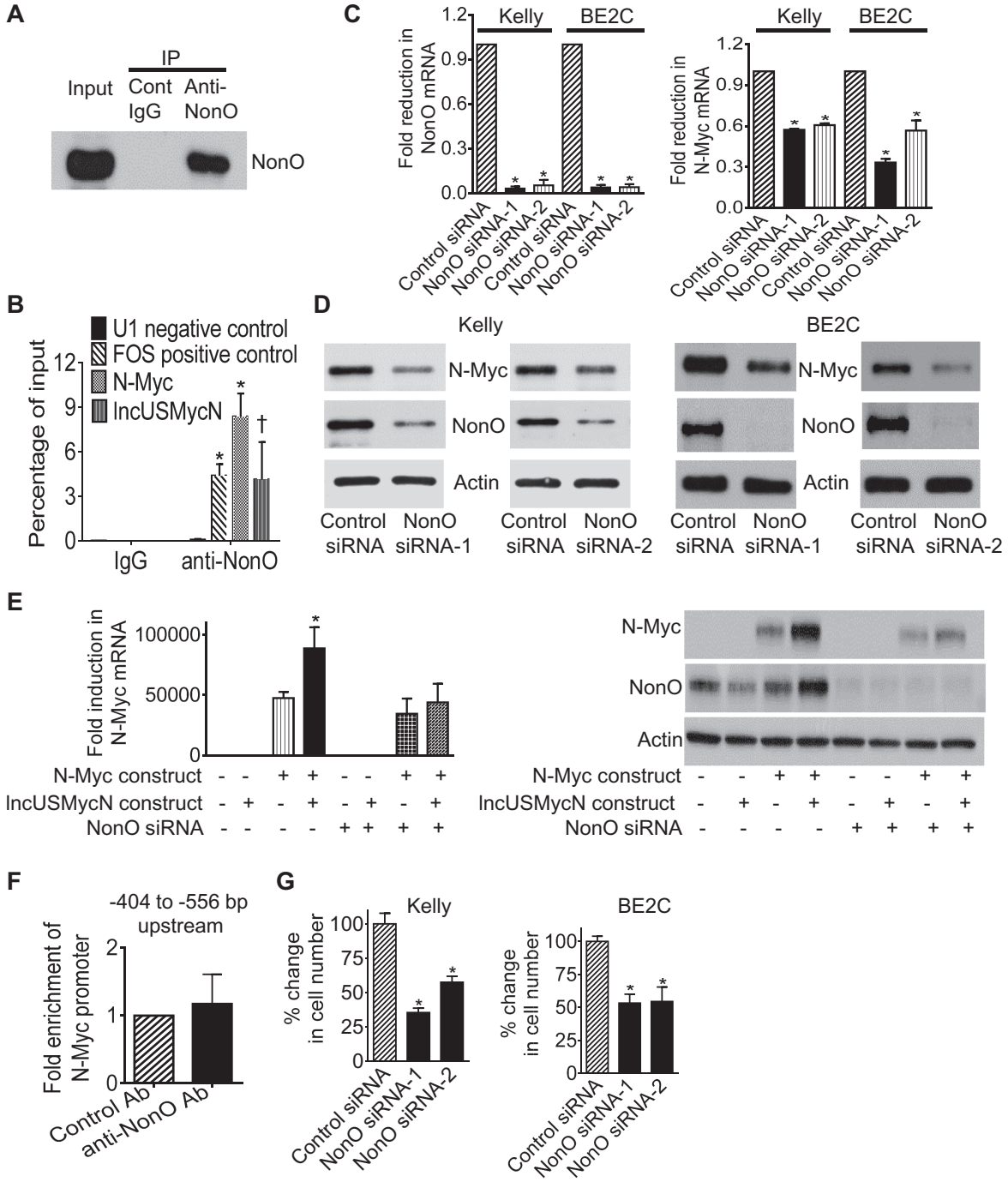

Figure 4. Modulation of N-Myc mRNA expression by the interaction between lncUSMycN and NonO. **A**) RNA immunoprecipitation assays were performed with a control or an anti-NonO antibody in Kelly cells. Immunoprecipitated protein was subjected to immunoblot analysis with the anti-NonO antibody. **B**) RNA samples immunoprecipitated by the control immunoglobulin G (IgG) or the anti-NonO antibody were subjected to reverse-transcription polymerase chain reaction (RT-PCR) analysis of lncUSMycN, N-Myc, the positive control FOS, or the negative control U1. One-way analysis of variance (ANOVA) was used to determine statistical significance. **C** and **D**) Kelly and BE2C cells were transfected with control siRNA, NonO siRNA-1, or NonO siRNA-2 for 48 hours, followed by RT-PCR (**C**) and immunoblot (**D**) analysis of NonO and N-Myc mRNA and protein expression. One-way ANOVA was used to determine statistical significance. **E**) *MYCN*-nonamplified SK-N-AS cells were transfected with control siRNA or NonO siRNA-1. Twenty-four hours later, the cells were cotransfected with an empty vector or lncUSMycN expression construct, together with an empty vector or N-Myc expression construct. N-Myc mRNA and protein expression was analysed by RT-PCR and immunoblot. One-way ANOVA was used to determine statistical significance. **F**) Chromatin immunoprecipitation assays were performed in Kelly cells with a control antibody (Ab) or an anti-NonO Ab and real-time PCR with primers targeting the proximal *MYCN* gene promoter (–404 to –556bp upstream of the *MYCN* gene transcription start site). Fold enrichment by control Ab was artificially set as 1.0. **G**) Kelly and BE2C cells were transfected with control siRNA, NonO siRNA-1, or NonO siRNA-2 for 96 hours. Relative cell numbers were examined by Alamar blue assays and expressed as percentage change in cell numbers. One-way ANOVA was used to determine statistical significance. Error bars represent standard deviation. *$P < .001$; †$P < .05$.

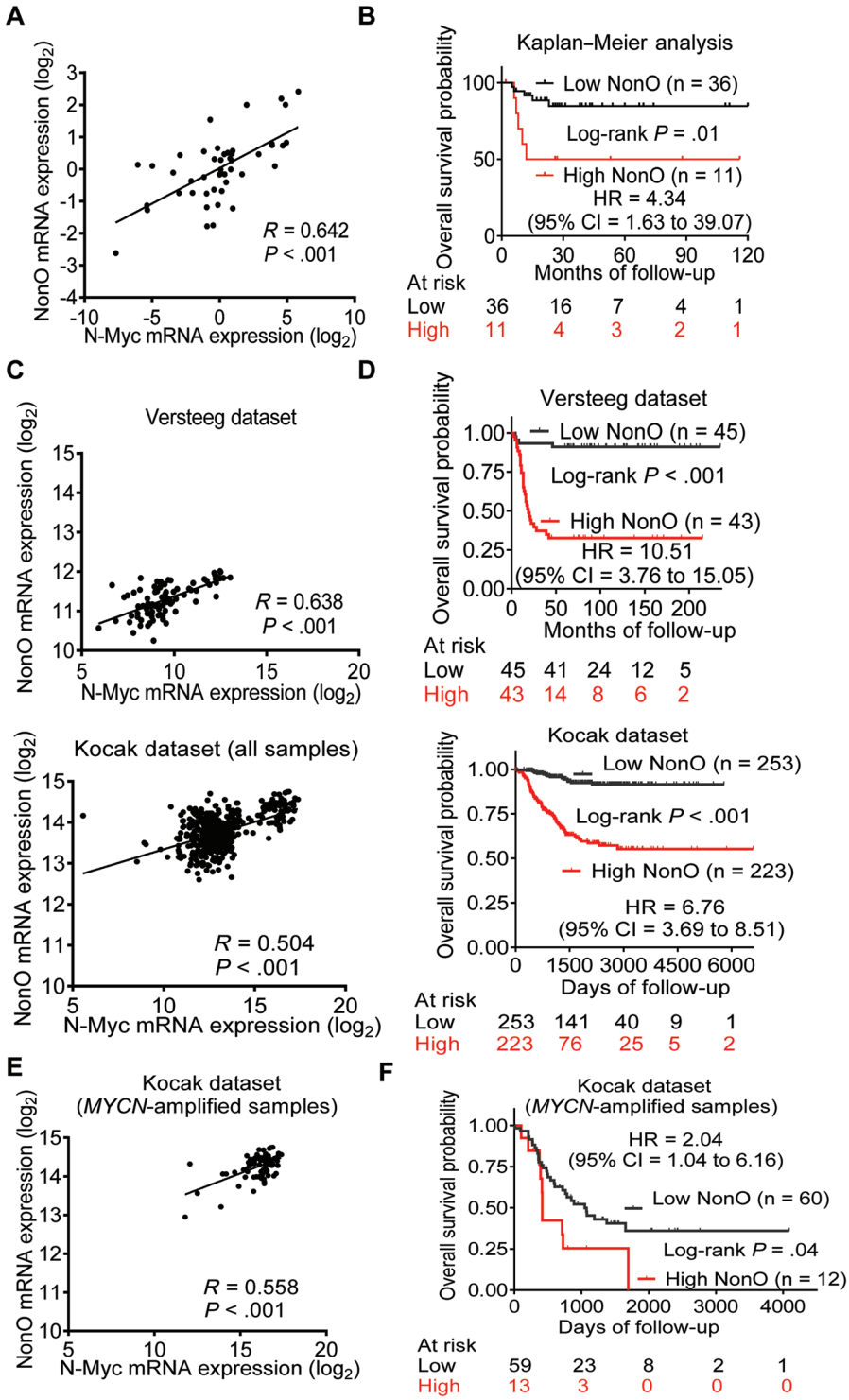

Figure 5. NonO in neuroblastoma cell proliferation and as a prognostic marker. **A**) Reverse-transcription polymerase chain reaction (RT-PCR) studies were performed in 47 human neuroblastoma cDNA samples with primers targeting NonO, N-Myc, or the loading control actin. Correlation between NonO expression and N-Myc expression in the tumor tissues was analyzed by two-sided Pearson's correlation. **B**) Kaplan–Meier curves showed the probability of overall survival of neuroblastoma patients according to the level of NonO expression in the 47 neuroblastoma patients. *P* value was obtained from two-sided log-rank test. **C**) Two-sided Pearson's correlation was used to analyze correlation between NonO expression and N-Myc expression in 88 and 476 human neuroblastoma samples in the publically available microarray gene expression Versteeg dataset and Kocak dataset, respectively, downloaded from R2 microarray analysis and visualization platform (http://r2.amc.nl, last accessed August 26, 2013). **D**) Kaplan–Meier curves showed the probability of overall survival of patients according to the levels of NonO expression in the 88 and 476 neuroblastoma patients in the Versteeg and Kocak datasets, respectively. *P* value was obtained from two-sided log-rank test. **E**) Two-sided Pearson's correlation was used to analyze correlation between NonO mRNA expression and N-Myc mRNA expression in 72 *MYCN* oncogene-amplified human neuroblastoma samples, which were a part of the 476 tumor samples in the publically available microarray gene expression Kocak dataset. **F**) Kaplan–Meier curves showed the probability of overall survival of patients according to the level of NonO expression in the 72 *MYCN* oncogene-amplified human neuroblastoma samples. CI = confidence interval; HR = hazard ratio. *P* value was obtained from two-sided log-rank test.

Modulation of N-Myc mRNA Expression by the Interaction Between lncUSMycN and NonO

To identify the mechanism by which lncUSMycN increased N-Myc mRNA expression, we in vitro transcribed lncUSMycN RNA from the pcDNA3.1-lncUSMycN expression construct and labeled the RNA with biotin, followed by incubation with Kelly cell protein lysates. Mass spectrometry analyses showed that lncUSMycN RNA specifically bound to proteins, including KHSRP, hnRNPU, FUBP1, and NonO (Supplementary Table 4, available online). RT-PCR studies showed that knocking down the expression of NonO, but not KHSRP, hnRNPU or FUBP1, modulated N-Myc mRNA expression (Supplementary Figure 4, available online).

We next performed RNA immunoprecipitation assays with an anti-NonO antibody or control antibody and Kelly cell lysates. Immunoblot and RT-PCR analyses showed that the NonO antibody indeed pulled down NonO protein (Figure 4A) and efficiently pulled down lncUSMycN RNA, N-Myc RNA, and the positive control FOS RNA, but not the negative control U1 RNA (Figure 4B).

We then transfected Kelly and BE2C cells with control siRNA, NonO siRNA-1, or NonO siRNA-2. RT-PCR and immunoblot analyses showed that NonO siRNAs reduced N-Myc mRNA expression in Kelly (mean fold of control ± SD: NonO siRNA-1, 0.57 ± 0.01; NonO siRNA-2, 0.61 ± 0.01) and BE2C cells (mean fold of control ± SD: NonO siRNA-1, 0.33 ± 0.03; NonO siRNA-2, 0.57 ± 0.07; $P < .001$, one-way ANOVA) (Figure 4C), and decreased N-Myc protein expression (Figure 4D). We next transfected SK-N-AS cells with control siRNA or NonO siRNA-1, followed by cotransfection with an N-Myc–expressing construct and/or a lncUSMycN-expressing construct. RT-PCR and immunoblot analysis showed that the lncUSMycN expression construct increased N-Myc mRNA and protein expression in cells cotransfected with control siRNA, but not in cells cotransfected with NonO siRNA-1 (Figure 4E; Supplementary Figure 4E, available online). Moreover, chromatin immunoprecipitation assays showed that immunoprecipitation with an anti-NonO antibody did not enrich DNA fragments at the *MYCN* gene promoter (Figure 4F), and Alamar blue assays revealed that NonO siRNAs reduced proliferation in Kelly and BE2C cells (Figure 4G). Taken together, the data indicate that NonO protein binds to lncUSMycN RNA and N-Myc RNA, upregulates N-Myc expression, and induces neuroblastoma cell proliferation and that lncUSMycN upregulates N-Myc mRNA expression by binding to NonO protein.

Prognostic Significance of NonO Expression in Primary Neuroblastoma

We next examined NonO mRNA expression in the cohort of 47 neuroblastoma cDNA samples (Supplementary Table 1, available online). RT-PCR analysis revealed that NonO mRNA expression correlated with N-Myc mRNA expression ($R = 0.642$; 95% CI = 0.437 to 0.783; $P < .001$) (Figure 5A), and Kaplan–Meier analysis showed that high levels of NonO mRNA expression in tumor tissues associated with poor patient prognosis (HR = 4.34; 95% CI = 1.63 to 39.07; $P = .01$) (Figure 5B). Consistently, the publicly available (http://r2.amc.nl, last accessed August 26, 2013) Versteeg and Kocak (19,20) microarray gene expression datasets from 88 and 476 patients both showed that NonO mRNA expression in human neuroblastoma tissues correlated with N-Myc mRNA expression (Versteeg dataset: $R = 0.638$, 95% CI = 0.494 to 0.747, $P < .001$; Kocak dataset: $R = 0.504$, 95% CI = 0.434 to 0.568, $P < .001$) (Figure 5C) and that high levels of NonO mRNA expression in tumor tissues associated with poor patient prognoses, using the mean of NonO expression as cut points (Versteeg dataset: HR = 10.51, 95% CI = 3.76 to 15.05, $P < .001$; Kocak dataset: HR = 6.76, 95% CI = 3.69 to 8.51, $P < .001$) (Figure 5D). Importantly, in the 72 *MYCN*-amplified human neuroblastoma tissues of the Kocak dataset, NonO mRNA expression also correlated with N-Myc mRNA expression ($R = 0.558$; 95% CI = 0.375 to 0.700; $P < .001$) (Figure 5E), and high levels of NonO mRNA expression in tumor tissues associated with poor patient prognosis (HR = 2.04; 95% CI = 1.04 to 6.16; $P = .04$) (Figure 5F). Additionally, high levels of lncUSMycN and NonO expression in neuroblastoma tissues strongly associated with reduced overall survival, independent of disease stage, age at the time of diagnosis, and *MYCN* oncogene amplification (lncUSMycN: HR = 1.87, 95% CI = 1.06 to 3.28, $P = .03$; NonO, HR = 2.48, 95% CI = 1.34 to 4.57, $P = .004$; multivariable Cox regression and two-sided log-rank test) (Table 1). Consistently, high levels of lncUSMycN expression in neuroblastoma tissues positively associated with reduced overall survival in 404 *MYCN*-nonamplified patients of the Kocak dataset (HR = 2.00; 95% CI = 1.05 to 5.65; $P = .04$) (Supplementary Figure 5, available online).

lncUSMycN Expression and Neuroblastoma Progression in Mice

We next designed LNA-ASO (31) targeting lncUSMycN (lncUSMycN LNA-ASO) and control LNA-ASO. RT-PCR studies confirmed that transfection with lncUSMycN LNA-ASO efficiently reduced lncUSMycN RNA expression in Kelly and BE2C neuroblastoma cells (Figure 6A). Consistent with data from lncUSMycN siRNAs, lncUSMycN LNA-ASO statistically significantly reduced N-Myc mRNA and protein expression, as well as proliferation in neuroblastoma cells (Figure 6, B and C).

We then xenografted Kelly neuroblastoma cells into nude mice and treated the mice with lncUSMycN LNA-ASO (n = 12

Table 1. Multivariable Cox regression analysis of factors prognostic for outcome in 476 neuroblastoma patients*

Factor	Overall survival (No. of deaths = 91) Hazard ratio (95% confidence interval)	*P*
High lncUSMyN expression	1.87 (1.06 to 3.28)	.03
High NonO expression	2.48 (1.34 to 4.57)	.004
Stage 4†	3.35 (2.01 to 5.61)	<.001
Age >12 mo	2.70 (1.38 to 5.28)	.004
MYCN gene amplification	2.26 (1.23 to 4.16)	.008

* The level of lncUSMycN and NonO expression was considered high or low in relation to the mean level of expression in all tumors analyzed. Hazard ratios were calculated as the antilogs of the regression coefficients in the proportional hazards regression. Multivariable Cox regression analysis was performed following the inclusion of the five above listed factors into the Cox regression model, and *P* value was obtained from two-sided log-rank test.

† Tumor stage was categorized as favorable (International Neuroblastoma Staging System stages 1, 2, 3 and 4S) or unfavorable (International Neuroblastoma Staging System stage 4) (22).

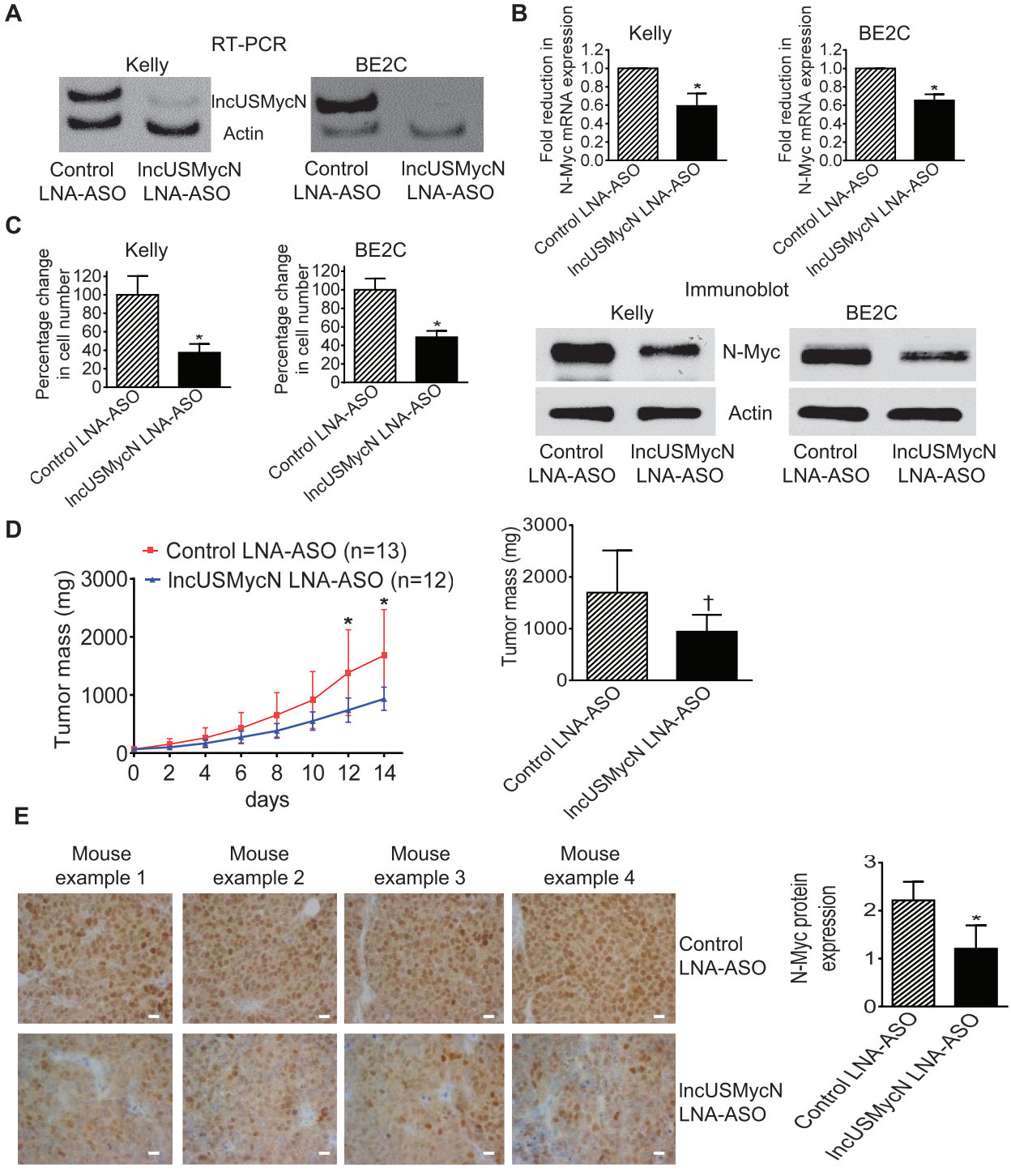

Figure 6. lncUSMycN expression and neuroblastoma progression in mice. **A**) Kelly and BE2C cells were transfected with control locked nucleic acid antisense oligonucleotides (LNA-ASO) or lncUSMycN LNA-ASO for 48 hours, followed by reverse-transcription polymerase chain reaction (RT-PCR) analysis of lncUSMycN expression. **B**) Kelly and BE2C cells were transfected with control LNA-ASO or lncUSMycN LNA-ASO for 48 hours, followed by RT-PCR and immunoblot analysis of N-Myc expression. Two-sided *t* test was used to determine statistical significance. **C**) Kelly and BE2C cells were transfected with control LNA-ASO or lncUSMycN LNA-ASO for 96 hours. Relative cell numbers were examined by Alamar blue assays and expressed as percentage changes in cell numbers. Two-sided *t* test was used to determine statistical significance. **D**) Kelly neuroblastoma cells were xenografted into nude mice. When tumor masses reached 0.05 g, the mice were injected intraperitoneally with control LNA-ASO (n = 13 mice) or lncUSMycN LNA-ASO (n = 12 mice) at 50 mg/kg every second day for 2 weeks. For the **left panel**, tumor masses were monitored in live mice every second day, and multiple-comparison two-way analysis of variance was used to determine statistical significance. For the **right panel**, tumors were weighed after the mice were killed, and two-sided *t* test was used to determine statistical significance. **E**) Tumor tissues from four mice treated with control LNA-ASO or lncUSMycN LNA-ASO were immunostained with an anti-N-Myc antibody and visualized with diaminobenzidine (**brown**). The nuclei were counterstained with hematoxylin (**blue**). N-Myc protein expression was semiquantified and expressed as histology scores. Two-sided *t* test was used to determine statistical significance. Scale bars represent 10 μm. Error bars represent standard deviation. **P* < .001; †*P* < .05.

mice) or control LNA-ASO (n = 13 mice). As shown in Figure 6D, treatment with lncUSMycN LNA-ASO statistically significantly reduced neuroblastoma mass (mean tumor mass ± SD: day 12, control LNA-ASO, 1384.47 ± 737.57 mg vs lncUSMycN LNA-ASO, 739.30 ± 327.12 mg; day 14, control LNA-ASO, 1682.97 ± 786.94 mg vs lncUSMycN LNA-ASO, 934.94 ± 299.36 mg; $P < .001$, multiple comparison two-way ANOVA). Immunohistochemistry analysis revealed that N-Myc protein was statistically significantly reduced by lncUSMycN LNA-ASO (mean N-Myc protein histology score ± SD: control LNA-ASO group, 2.22 ± 0.39 vs lncUSMycN LNA-ASO group, 1.21 ± 0.49 mg; $P < .001$, two-sided t test) (Figure 6E). These results therefore demonstrate that lncUSMycN plays an important role in neuroblastoma progression, at least partly through upregulating N-Myc expression.

Discussion

The lncRNA ncRAN acts like an oncogene in aggressive neuroblastoma (32), and the lncRNA transcribed ultraconserved regions are involved in diverse cellular processes, such as p53 response and proliferation, in neuroblastoma (33). Through examination of HAVANA bioinformatics data and biological experiments, we have identified a novel lncRNA, lncUSMycN, that is transcribed approximately 14 kb upstream of the *MYCN* transcription start site and have confirmed its three exons as well as its absence of protein-coding capacity. We have also demonstrated that the *lncUSMycN* and the *MYCN* genes are coamplified in approximately one-quarter of human neuroblastoma tissues and that a high level of lncUSMycN expression in human neuroblastoma tissues independently predicts poor patient prognosis.

lncRNAs are emerging as critical regulators of gene expression through transcriptional and post-transcriptional mechanisms. For example, the antisense lncRNA HOTAIR (34,35), Air, Kcnq1ot1 (36,37), Evx1AS, and HoxB5/B6AS (38) regulate gene expression by binding to histone modifying enzymes or transcription factors. Sense lncRNAs upregulate the transcription of their neighboring protein-coding genes by interacting with WDR5 or Mediator (11,14,29). In this study, we found that knocking down lncUSMycN expression with siRNAs reduces N-Myc mRNA and protein expression in *MYCN* oncogene-amplified neuroblastoma cells and that ectopic lncUSMycN expression in *MYCN*-nonamplified neuroblastoma cells increases exogenous N-Myc mRNA and protein expression. Because knocking down lncUSMycN expression does not affect the presence of trimethyl-H3K4 at the *MYCN* gene promoter, lncUSMycN upregulates N-Myc expression through a post-transcriptional mechanism.

Myc oncoproteins are well known to exert tumorigenic effects through inducing cell proliferation (39,40). In this study, analysis of lncUSMycN expression in neuroblastoma cells shows that lncUSMycN is expressed at the highest levels at G1/S and S phases of the cell cycle, and cell proliferation assays confirm that knocking down lncUSMycN expression in neuroblastoma cells results in growth inhibition. Importantly, this study further shows that knocking down lncUSMycN expression reduces N-Myc expression in tumor tissues and hinders tumor progression in neuroblastoma-bearing mice. Taken together, our in vitro and in vivo data suggest that lncUSMycN plays important roles in N-Myc expression, cell proliferation, and tumorigenesis and that lncUSMycN is a novel target for the therapy of neuroblastoma.

In this study, we have identified NonO as one of the proteins bound to lncUSMycN RNA. NonO enhances mRNA maturation (41), regulates mRNA nuclear retention and post-transcriptional processing (42–44), and upregulates mRNAs through binding to Sox9 or Instability Elements (41,45). This study shows that NonO binds to both lncUSMycN RNA and N-Myc RNA and that silencing NonO expression blocks lncUSMycN-induced N-Myc mRNA and protein overexpression. Our data indicate that lncUSMycN increases N-Myc mRNA expression through binding to NonO, which post-transcriptionally upregulates N-Myc expression. Importantly, this study further confirms that a high level of NonO expression in human neuroblastoma tissues correlates with a high level of N-Myc expression, advanced disease stage, and poor prognosis. These data therefore demonstrate that a high level of NonO expression in human neuroblastoma tissues can be used as a marker for poor prognosis and that NonO is a novel therapeutic target.

A limitation of this study is the lack of therapeutic application of the discoveries at the moment. Future studies are required to identify clinically applicable small molecule compounds that block the interaction between lncUSMycN and NonO and reduce N-Myc expression and neuroblastoma progression.

References

1. Reiter JL, Brodeur GM. High-resolution mapping of a 130-kb core region of the MYCN amplicon in neuroblastomas. *Genomics*. 1996;32(1):97–103.
2. Gustafson WC, Weiss WA. Myc proteins as therapeutic targets. *Oncogene*. 2010;29(9):1249–1259.
3. Meyer N, Penn LZ. Reflecting on 25 years with MYC. *Nat Rev Cancer*. 2008;8(12):976–990.
4. Brodeur GM. Neuroblastoma: biological insights into a clinical enigma. *Nat Rev Cancer*. 2003;3(3):203–216.
5. Mercer TR, Dinger ME, Mattick JS. Long non-coding RNAs: insights into functions. *Nat Rev Genet*. 2009;10(3):155–159.
6. Amaral PP, Dinger ME, Mercer TR, Mattick JS. The eukaryotic genome as an RNA machine. *Science*. 2008;319(5871):1787–1789.
7. Guttman M, Amit I, Garber M, et al. Chromatin signature reveals over a thousand highly conserved large non-coding RNAs in mammals. *Nature*. 2009;458(7235):223–227.
8. Mercer TR, Mattick JS. Structure and function of long noncoding RNAs in epigenetic regulation. *Nat Struct Mol Biol*. 2013;20(3):300–307.
9. Batista PJ, Chang HY. Long noncoding RNAs: cellular address codes in development and disease. *Cell*. 2013;152(6):1298–1307.
10. Takayama KI, Horie-Inoue K, Katayama S, et al. Androgen-responsive long noncoding RNA CTBP1-AS promotes prostate cancer. *EMBO J*. 2013;32(12):1665–1680.
11. Orom UA, Derrien T, Beringer M, et al. Long noncoding RNAs with enhancer-like function in human cells. *Cell*. 2010;143(1):46–58.
12. Tripathi V, Shen Z, Chakraborty A, et al. Long noncoding RNA MALAT1 controls cell cycle progression by regulating the expression of oncogenic transcription factor B-MYB. *PLoS Genet*. 2013;9(3):e1003368.
13. Johnsson P, Ackley A, Vidarsdottir L, et al. A pseudogene long-noncoding-RNA network regulates PTEN transcription and translation in human cells. *Nat Struct Mol Biol*. 2013;20(4):440–446.
14. Wang KC, Yang YW, Liu B, et al. A long noncoding RNA maintains active chromatin to coordinate homeotic gene expression. *Nature*. 2011;472(7341):120–124.
15. Gupta RA, Shah N, Wang KC, et al. Long non-coding RNA HOTAIR reprograms chromatin state to promote cancer metastasis. *Nature*. 2010;464(7291):1071–1076.
16. Mattick JS. The genetic signatures of noncoding RNAs. *PLoS Genet*. 2009;5(4):e1000459.

17. Taft RJ, Pang KC, Mercer TR, Dinger M, Mattick JS. Non-coding RNAs: regulators of disease. *J Pathol*. 2010;220(2):126–139.
18. Cheung B, Hocker JE, Smith SA, Norris MD, Haber M, Marshall GM. Favorable prognostic significance of high-level retinoic acid receptor beta expression in neuroblastoma mediated by effects on cell cycle regulation. *Oncogene*. 1998;17(6):751–759.
19. Kocak H, Ackermann S, Hero B, et al. Hox-C9 activates the intrinsic pathway of apoptosis and is associated with spontaneous regression in neuroblastoma. *Cell Death Dis*. 2013;4(4):e586.
20. Oberthuer A, Juraeva D, Li L, et al. Comparison of performance of one-color and two-color gene-expression analyses in predicting clinical endpoints of neuroblastoma patients. *Pharmacogenomics J*. 2010;10(4):258–266.
21. Kaplan EL, Meier P. Nonparametric estimation from incomplete observations. In: Kotz S, Johnson N, eds. *Breakthroughs in Statistics*. Springer: New York; 1992:319–337.
22. Brodeur GM, Seeger RC, Barrett A, et al. International criteria for diagnosis, staging, and response to treatment in patients with neuroblastoma. *J Clin Oncol*. 1988;6(12):1874–1881.
23. Marshall GM, Liu PY, Gherardi S, et al. SIRT1 promotes N-Myc oncogenesis through a positive feedback loop involving the effects of MKP3 and ERK on N-Myc protein stability. *PLoS Genet*. 2011;7(6):e1002135.
24. Liu PY, Xu N, Malyukova A, et al. The histone deacetylase SIRT2 stabilizes Myc oncoproteins. *Cell Death Differ*. 2013;20(3):503–514.
25. Liu T, Tee AE, Porro A, et al. Activation of tissue transglutaminase transcription by histone deacetylase inhibition as a therapeutic approach for Myc oncogenesis. *Proc Natl Acad Sci U S A*. 2007;104(47):18682–18687.
26. Liu T, Liu PY, Tee AE, et al. Over-expression of clusterin is a resistance factor to the anti-cancer effect of histone deacetylase inhibitors. *Eur J Cancer*. 2009;45(10):1846–1854.
27. Ling D, Marshall GM, Liu PY, et al. Enhancing the anticancer effect of the histone deacetylase inhibitor by activating transglutaminase. *Eur J Cancer*. 2012;48(17):3278–3287.
28. Kuljaca S, Liu T, Dwarte T, et al. The cyclin-dependent kinase inhibitor, p21(WAF1), promotes angiogenesis by repressing gene transcription of thioredoxin-binding protein 2 in cancer cells. *Carcinogenesis*. 2009;30(11):1865–1871.
29. Lai F, Orom UA, Cesaroni M, et al. Activating RNAs associate with Mediator to enhance chromatin architecture and transcription. *Nature*. 2013;494(7438):497–501.
30. Bell JL, Malyukova A, Kavallaris M, Marshall GM, Cheung BB. TRIM16 inhibits neuroblastoma cell proliferation through cell cycle regulation and dynamic nuclear localization. *Cell Cycle*. 2013;12(6):889–898.
31. Straarup EM, Fisker N, Hedtjarn M, et al. Short locked nucleic acid antisense oligonucleotides potently reduce apolipoprotein B mRNA and serum cholesterol in mice and non-human primates. *Nucleic Acids Res*. 2010;38(20):7100–7111.
32. Yu M, Ohira M, Li Y, et al. High expression of ncRAN, a novel non-coding RNA mapped to chromosome 17q25.1, is associated with poor prognosis in neuroblastoma. *Int J Oncol*. 2009;34(4):931–938.
33. Mestdagh P, Fredlund E, Pattyn F, et al. An integrative genomics screen uncovers ncRNA T-UCR functions in neuroblastoma tumours. *Oncogene*. 2010;29(24):3583–3592.
34. Tsai MC, Manor O, Wan Y, et al. Long noncoding RNA as modular scaffold of histone modification complexes. *Science*. 2010;329(5992):689–693.
35. Rinn JL, Kertesz M, Wang JK, et al. Functional demarcation of active and silent chromatin domains in human HOX loci by noncoding RNAs. *Cell*. 2007;129(7):1311–1323.
36. Nagano T, Mitchell JA, Sanz LA, et al. The Air noncoding RNA epigenetically silences transcription by targeting G9a to chromatin. *Science*. 2008;322(5908):1717–1720.
37. Pandey RR, Mondal T, Mohammad F, et al. Kcnq1ot1 antisense noncoding RNA mediates lineage-specific transcriptional silencing through chromatin-level regulation. *Mol Cell*. 2008;32(2):232–246.
38. Dinger ME, Amaral PP, Mercer TR, et al. Long noncoding RNAs in mouse embryonic stem cell pluripotency and differentiation. *Genome Res*. 2008;18(9):1433–1445.
39. Eilers M, Eisenman RN. Myc's broad reach. *Genes Dev*. 2008;22(20):2755–2766.
40. Dang CV. MYC on the path to cancer. *Cell*. 2013;149(1):22–35.
41. Hata K, Nishimura R, Muramatsu S, et al. Paraspeckle protein p54nrb links Sox9-mediated transcription with RNA processing during chondrogenesis in mice. *J Clin Invest*. 2008;118(9):3098–3108.
42. Zhang Z, Carmichael GG. The fate of dsRNA in the nucleus: a p54(nrb)-containing complex mediates the nuclear retention of promiscuously A-to-I edited RNAs. *Cell*. 2001;106(4):465–475.
43. Chen LL, Carmichael GG. Altered nuclear retention of mRNAs containing inverted repeats in human embryonic stem cells: functional role of a nuclear noncoding RNA. *Mol Cell*. 2009;35(4):467–478.
44. Prasanth KV, Prasanth SG, Xuan Z, et al. Regulating gene expression through RNA nuclear retention. *Cell*. 2005;123(2):249–263.
45. Zolotukhin AS, Michalowski D, Bear J, et al. PSF acts through the human immunodeficiency virus type 1 mRNA instability elements to regulate virus expression. *Mol Cell Biol*. 2003;23(18):6618–6630.

Funding

The authors were supported by National Health & Medical Research Council (NHMRC), Italian Association for Research on Cancer, Cancer Institute New South Wales and Cancer Council New South Wales grants. TL is a recipient of an Australian Research Council Future Fellowship.

Notes

Children's Cancer Institute Australia is affiliated with University of New South Wales and Sydney Children's Hospital. The funders did not have any involvement in the design of the study; the collection, analysis and interpretation of the data; the writing of the manuscript; and the decision to submit the manuscript for publication.

Affiliations of authors: Children's Cancer Institute Australia for Medical Research, Randwick NSW, Australia (PYL, GMM, AET, MW, BL, BBC, MK, TL); Department of Pharmacy and Biotechnology, University of Bologna, Bologna, Italy (DE, GM, GP); Kids Cancer Centre, Sydney Children's Hospital, Randwick NSW, Australia (GMM); Department of Pathology and Inflammation and Infection Research Centre, University of New South Wales, Kensington 2052, Australia (PP); Institute of Molecular Medicine, Martin Luther University, ZAMED, Halle, Germany (JLB, SH); School of Medicine and Public Health, Priority Research Centre for Cancer Research, University of Newcastle, Callaghan NSW, Australia (XDZ); Harry Perkins Institute of Medical Research, Centre for Medical Research, University of Western Australia, Nedlands WA, Australia (AF); Kinghorn Cancer Centre and Cancer Research Division, Garvan Institute of Medical Research, Darlinghurst NSW, Australia (AS); St Vincent's Clinical School, University of New South Wales, Darlinghurst NSW, Australia (AS, JSM, MED); Australian Centre for Nanomedicine, Randwick NSW, Australia (MK); Garvan Institute of Medical Research, Darlinghurst NSW, Australia (AS, JSM, MED); School of Women's & Children's Health, University of New South Wales, Randwick NSW, Australia (TL).